ENVIRONMENTAL RESEARCH
COMMUNICATIONS

INCLUSIVE PUBLISHING TRUSTED SCIENCE

Part of the ENVIRONMENTAL RESEARCH SERIES

PURPOSE-LED PUBLISHING™

PAPER • OPEN ACCESS

Maps are good but are simpler maps better? Insights on urban bicycling in the US

To cite this article: Mohammed Abdalazeem *et al* 2026 *Environ. Res. Commun.* **8** 025004

Environmental Research Communications

Check for updates

OPEN ACCESS

RECEIVED
2 September 2025

REVISED
31 December 2025

ACCEPTED FOR PUBLICATION
15 January 2026

PUBLISHED
4 February 2026

PAPER

Maps are good but are simpler maps better? Insights on urban bicycling in the US

Mohammed Abdalazeem[1], **Geehan Altayb**[2], **Eleni Christofa**[1] and **Jimi Oke**[1,*]

[1] Department of Civil and Environmental Engineering, University of Massachusetts, Amherst, MA, United States of America
[2] Department of Computer Science, Howard University, Washington DC, United States of America
[*] Author to whom any correspondence should be addressed.

E-mail: jimi@umass.edu

Keywords: bicycle maps, typology analysis, bicycle usage, spatial analysis, urban analytics, interpretable machine learning, SHapley Additive exPlanations (SHAP)

Abstract

Bicycles are critical to health and sustainability, and promise to play a key role in the decarbonization of passenger transportation worldwide. Yet, while infrastructure investments are well studied, the relationship between bicycle maps (availability and features) and bicycle usage remains largely unexamined. Using the United States as a case study, we surveyed 684 urban counties, finding that only 45% have publicly available bicycle maps online. From these maps, we observed five features: *Level of Infrastructure*, *Amenity Locations*, *Level of Stress*, *Transit Locations*, and *Interactive* features. Based on these binary features, we clustered the counties via a Bernoulli mixture model to obtain a typology of three map types. Then using socioeconomic indicators from the American Community Survey as predictors, along with map-related features, we fitted three XGBoost models to predict county-level bicycle mode share, with R^2_{test} ranging from 0.45 to 0.58, indicating moderate explanatory power. The models indicate that map availability has a positive association with bicycle usage. Furthermore, we find that detailed maps are associated with lower bicycle usage, while the reverse is the case for simple maps. Finally, of the 5 map features identified, *Level of Infrastructure* and *Transit Locations* are the most relevant in explaining bicycle usage but with a negative association. Ultimately, producing maps that emphasize simple and legible design may represent a low-cost strategy to complement infrastructure investments and promote bicycle usage for healthier communities and climate change mitigation.

1. Introduction

Bicycling offers substantial benefits for sustainability, health and quality of life [1]. Amid the climate change crisis, bicycles promise to play a key role in the decarbonization of passenger transportation, given their potential to replace passenger cars on short-distance trips, particularly in dense urban areas [2–4]. The potential for the realization of this mitigation pathway is particularly high in a country such as the United States, which has the world's highest per-capita car ownership rate (0.8), but only moderately high bicycle ownership (also 0.8 per capita) by global standards (the highest being 1.2 per capita)[4, 5]. Among similarly high-income nations, bicycle usage in the US, however, lags behind ownership rates [4]. Currently, US nationwide bicycle mode share is at just 1% [6, 7]. Meanwhile, countries such as Denmark and the Netherlands boast of bicycle mode shares of over 20%, while China's is at 10% [4]. This highlights the scale of the emissions mitigation potential of increased bicycle usage in the US.

Transportation psychology research demonstrates that mode choice decisions involve extensive information processing [8], with bicycling intentions significantly influenced by information interventions that improve perceived behavioral control [9–11]. Wayfinding studies show that spatial navigation is highly dependent on external information sources, with maps serving as critical guides that can be more influential than direct experience [12, 13]. Maps also communicate crucial safety information for bicycling decisions. Cyclists consistently prefer routes with clearly marked infrastructure and safety features [14–17], suggesting that visualizing infrastructure types and traffic stress levels through maps may directly influence perceptions of bicycling safety and route choice.

While research on bicycling behavior interventions has expanded in recent years, it has focused on other forms of information provision. Evidence from bicycling-related information campaigns indicates that message design can influence perceptions and perceived control, but behavioral impacts are mixed [11, 18]. Spatio-temporal analyses of bicycling have revealed pronounced daily and weekly rhythms and strong coupling with human activity patterns and the built environment, suggesting that the usefulness of map content depends on when and where trips occur [19–21]. Furthermore, cyclist preferences vary considerably, with some prioritizing direct routes while others seeking lower-traffic or scenic alternatives. Infrastructure data quality also remains a challenge, with automated audits revealing missing links and incomplete coverage even in data-rich contexts [22]. Existing studies investigating the factors influencing bicycling often focus primarily on physical infrastructure [23–26] or mapping precision [27, 28], leaving maps as an overlooked policy intervention.

The design and content of bicycle maps (in contrast with transit maps, for instance) present additional complexities that warrant investigation. Key features include representation of infrastructure levels (protected lanes, conventional lanes, sharrows), level of stress or safety information, transit connections, and amenity locations [29]. However, bicycle map design involves balancing detail with readability, as excessive information can overwhelm users, while oversimplification can omit crucial navigation data [29, 30]. Recent usability research indicates that adding bicycling-specific layers and detail can increase visual map complexity [31, 32]. Yet, investigations into whether map complexity (symbol density and legend organization) impairs wayfinding and degrades overall efficiency have been inconclusive [29, 32]. In parallel, cyclist-aware digital mapping has advanced in ways that clarify which layers are most decision-relevant, including cycle-specific map matching, surface-condition-aware routing, and related network modeling [33, 34]. Despite these advances, most public-sector bicycle maps are still static documents that do not incorporate such algorithmic sophistication, creating a gap between state-of-the-art navigation tools and government-provided map products [33]. These design considerations raise questions about which map features are the most prevalent and potentially most influential for bicycling behavior.

However, no research has directly tested whether there exists a significant relationship between the availability of bicycle maps and bicycle usage and, if so, which map characteristics or features are most relevant. Geographic disparities in bicycle usage compound this research gap, as there are substantial variations between jurisdictions in map availability and quality [30, 35]. These disparities have persisted despite extensive research and deployment of physical infrastructure interventions, suggesting that information barriers may play an underexplored role in bicycling adoption. Ultimately, while infrastructure provision and digital navigation tools have been widely studied, the influence of the design and availability of official bicycle maps on bicycle usage has yet to be systematically evaluated. This represents a significant knowledge gap, since maps constitute one of the most tangible and widely accessible forms of bicycling information that governments provide.

This study aims to address the aforementioned gaps by addressing three research questions: (1) How prevalent are publicly available bicycle maps across US urban counties? (2) What distinct types of bicycle maps can be identified based on their content and features? (3) To what extent are map availability and characteristics associated with bicycle mode share after accounting for socioeconomic factors? Our objectives were thus to estimate urban bicycle map availability in the US, develop a typology of bicycle maps based on key features, and investigate the nature of the relationship between map availability, along with observed map features, and bicycle usage. We find that only 45% of US urban counties have publicly available maps online. Our predictive models also indicate that the most detailed maps are associated with lower bicycle usage, while the reverse is the case for the simplest maps. Thus, our contribution isolates map simplification as a potential policy lever, in contrast with infrastructure-focused studies that estimate the effects of building new facilities [23–26] and accuracy-focused efforts aimed at improving the completeness and precision of bicycling networks [27, 28]. Whereas infrastructure expansion is capital-intensive and accuracy initiatives aim to correct what is shown, simplification targets how information is shown, which reduces visual complexity and facilitates decision-making. Because simplification can be implemented relatively quickly through design choices, it could offer near-term, low-cost leverage for agencies seeking to influence bicycling behavior.

2. Methods

First, we sampled 684 of the 1,186 urban counties in the US [36], conducting systematic online searches for publicly available bicycle maps. We then visually inspected each map to determine the presence of five key indicators: *Level of Infrastructure*, *Amenity Locations*, *Level of Stress*, *Transit Locations*, and *Interactive* features. Using these binary indicators, we fitted a Bernoulli mixture model via variational Bayes to identify three bicycle map types. We then estimated three gradient boosting models. The first investigated whether map availability was a relevant indicator for predicting bicycle mode share across the 684 counties in our sample. The second model examined the relationship

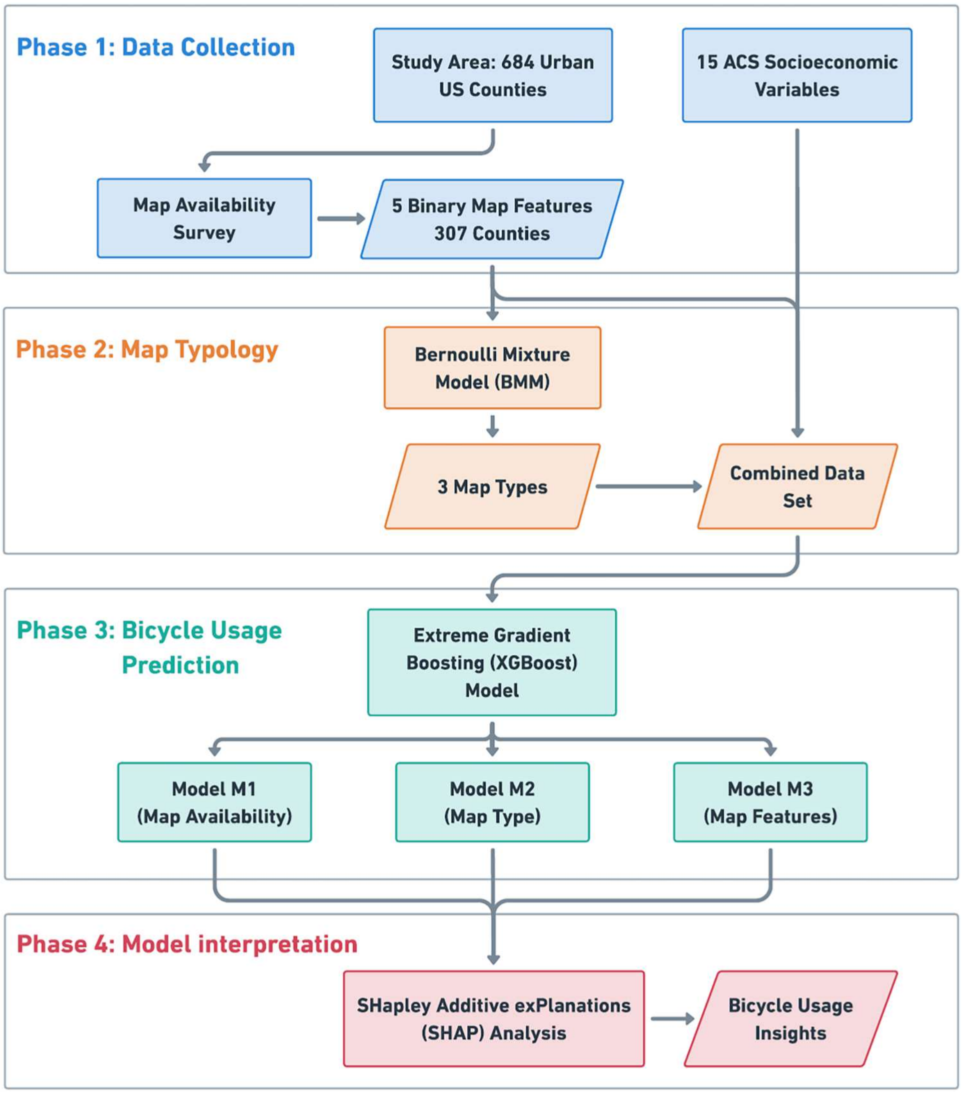

Figure 1. Flowchart depicting the framework of the study.

between map types and bicycle mode share using only the 307 counties with available maps. The third model analyzed which of the five binary features was most relevant to bicycle mode share. All models demonstrated moderate predictive power. They also critically indicated that map availability and features are relevant to explaining bicycle usage. Model interpretations yield potentially actionable insights into the role of simplified map designs in improving bicycling outcomes. The overall methodological framework is shown in figure 1.

2.1. Study area

We selected the US as the study area due to both its scale and the significant variability in its urban characteristics, geography and socioeconomics [37]. The US also exhibits substantial variability in bicycle usage, as bicycle mode shares range from under 0.1% to over 5% across its urban counties [7]. Map design and content vary similarly, as bicycle map creation is managed by individual municipalities and counties rather than via centralized standards. Our sample of 684 urban counties, drawn from the 1,186 counties classified as metropolitan areas [36], spans all major US regions and includes cities of varying sizes and urban forms. Furthermore, the US features a wealth of relevant county-level data that are consistently collected via the American Community Surveys (ACS). Together, these factors allow for the creation of a heterogeneous and representative dataset from which we can draw useful conclusions.

2.2. Map availability survey

We defined the sampling frame as the 1,186 urban U.S. counties designated by the U.S. Office of Management and Budget [36], treating the county as the unit of analysis. From this universe, we sampled 684 counties for manual web retrieval and coding of bicycle maps during the study window. A county was eligible if it (i) fell

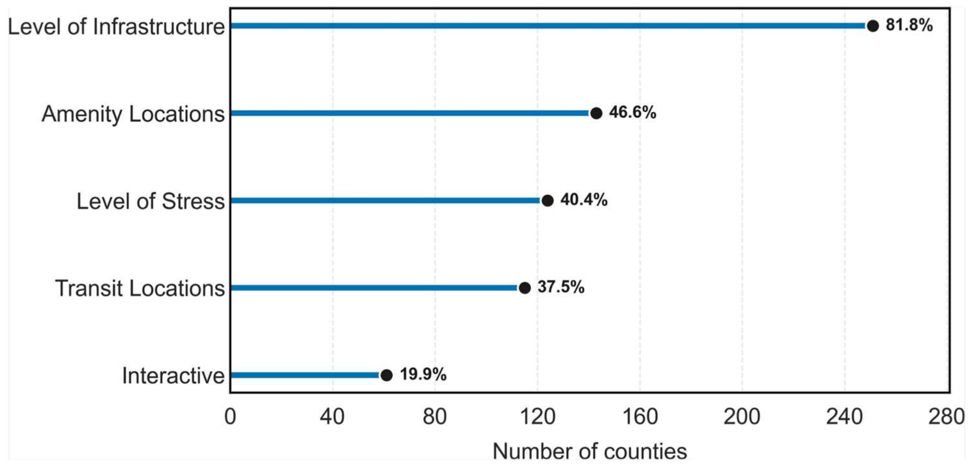

Figure 2. Summary of indicator averages across urban counties with maps available.

within the OMB-defined urban county universe and (ii) had an official county or principal city website (transportation or planning page) that could plausibly host a bicycle map (static or interactive). Counties without an identified map were labeled as 'Not Available.' In cases where a county included multiple municipalities, we marked the county as 'Available' if at least one official county- or city-operated bicycle map was found. This subset spans all Census regions and a wide range of urban contexts.

We searched online to identify publicly available bicycle maps in any format (such as portable document format and interactive web maps) for 684 urban counties in the US. For each county, we first queried Google using the strings '[county name] bicycle map' and '[county name] bike map.' When no official resource appeared, we manually checked the county or principal-city government website (Department of Transportation, planning, or sustainability pages). Publication dates were inconsistently reported across these maps, and thus age was not included as a variable.

2.3. Map feature identification

We then visually analyzed each map and labeled the five binary indicators: *Level of Infrastructure*, *Level of Stress*, *Amenity Locations*, *Transit Locations*, and *Interactive*. Two co-authors independently analyzed the maps and performed the labeling twice to ensure consistency and correctness. The labels reflect the state of the bicycle maps available online during our study window, which spanned July 2024 through May 2025. A summary of the indicators for the 307 county maps is shown in figure 2. Furthermore, a coding guide summarizing indicator definitions and example legend items is provided in appendix A.2.

Level of Infrastructure indicates whether the map displays information on different types of bicycling infrastructure, such as protected bicycle lanes, multi-use paths, shared-use paths, or conventional bicycle lanes. This feature was present in 81.8% of available maps, making it the most common element. *Level of Stress* refers to whether the map provides indicators of bicycling comfort or safety along routes, such as traffic stress levels, route difficulty ratings, or suitability classifications that help cyclists assess route conditions. This information appeared on 40.4% of the maps. *Amenity Locations* indicates whether the map includes bicycling-related amenities such as bicycle shops, repair stations, or bicycle parking facilities, and was found in 46.6% of maps. Similarly, *Transit Locations* refers to whether the map shows public transportation connections and was found in 37.5% of the maps, while *Interactive* indicates whether the map provides interactive features such as route planning capabilities, clickable elements for additional information, or zooming functions, which was available for 19.9% of the maps.

2.4. Bayesian Bernoulli mixture modeling

Based on the five binary feature indicators, we then clustered the maps using a Bernoulli mixture model (BMM) as follows. Given a set of D binary variables (map features) $\boldsymbol{x} = x_1, \ldots, x_D$, where $x_d \sim \text{Bernoulli}(\mu_d)$. We define $\boldsymbol{\mu} = (\mu_1, \ldots, \mu_D)^\top$ as the vector of Bernoulli parameters (probability of 1) for each of the variables. Thus,

$$p(\boldsymbol{x}|\boldsymbol{\mu}) = \prod_{d=1}^{D} \mu_d^{x_d}(1 - \mu_d)^{1-x_d} \tag{1}$$

We assume that each instance of $\boldsymbol{x}$ is generated by the latent binary variable $\boldsymbol{z} = (z_1, \ldots, z_K)^\top$. Thus, we specify the generative model (conditional and prior distributions) of the finite BMM as:

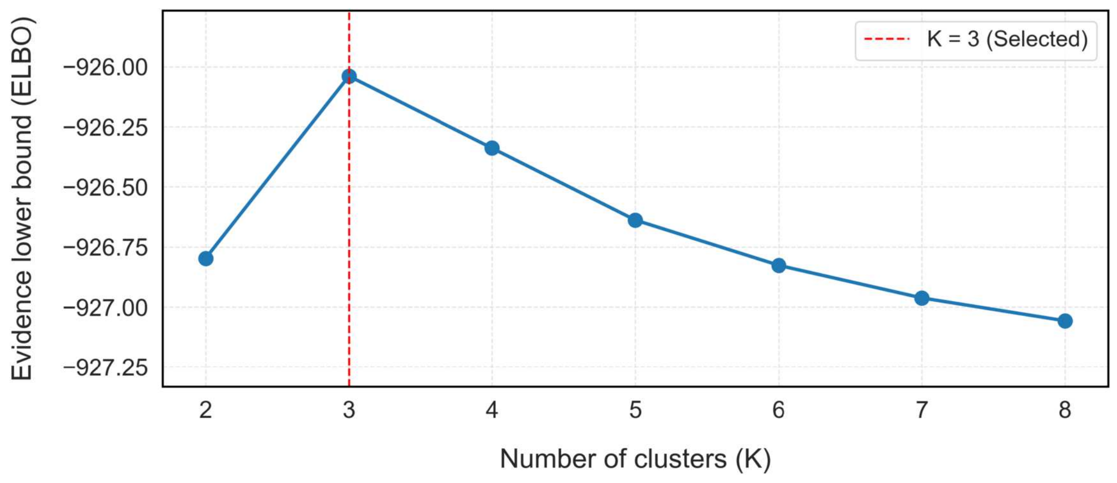

Figure 3. Evidence Lower Bound (ELBO) for variational Bayesian mixture models with $K \in \{2, \ldots, 8\}$ clusters. Each point represents the best ELBO achieved across 10 random initializations. The vertical dashed line indicates the chosen model with $K = 3$.

$$p(\boldsymbol{x}|\boldsymbol{z},\,\boldsymbol{\mu}) = \prod_{k=1}^{K} p(\boldsymbol{x}|\boldsymbol{\mu}_k)^{z_k} \tag{2}$$

$$p(\boldsymbol{z}|\boldsymbol{\pi}) = \prod_{k=1}^{K} \pi_k^{z_k} \tag{3}$$

where $\boldsymbol{\pi} = (\pi_1, \ldots, \pi_K)^\top$ is the vector of mixture weights or responsibilities (i.e., the probabilities of assignment to each cluster $1, \ldots K$).

In our case, we define μ_{dk} as the probability of the counties in the kth cluster with 1's in the dth feature, imposing a U-shaped Beta prior distribution ($\beta = 0.5$) [38]. The responsibilities, $\boldsymbol{\pi}$, are given uninformative Dirichlet priors ($\boldsymbol{\alpha} = 1 \times 10^{-5}\mathbf{I}_K$). $z_{nk} \in \{0, 1\}$ is the cluster assignment of county n and $x_{nd} \in \{0, 1\}$ indicates the presence of feature d for a map in county n. The complete model is specified as:

$$p(\boldsymbol{\mu}) = \prod_{k=1}^{K}\prod_{d=1}^{D} \mathcal{B}e(\mu_{dk}|\beta) \tag{4}$$

$$p(\boldsymbol{\pi}) = \mathrm{Dir}(\boldsymbol{\pi}|\boldsymbol{\alpha}) \tag{5}$$

$$p(\boldsymbol{Z}|\boldsymbol{\pi}) = \prod_{n=1}^{N}\prod_{k=1}^{K} \pi_k^{z_{nk}} \tag{6}$$

$$p(\boldsymbol{X}|\boldsymbol{Z},\,\boldsymbol{\mu}) = \prod_{n=1}^{N}\prod_{k=1}^{K}\left(\prod_{d=1}^{D} \mu_{dk}^{x_{dn}}(1 - \mu_{dk})^{(1-x_{dn})}\right)^{z_{kn}} \tag{7}$$

for $d \in \{1, \ldots, 8\}$, $k \in \{1, \ldots, K\}$ and $n \in \{1, \ldots, N\}$. We set $\boldsymbol{\alpha} = 1 \times 10^{-5}\mathbf{I}_K$ and $\beta = 0.5$. The complete data likelihood is given by

$$p(\boldsymbol{X},\,\boldsymbol{Z},\,\boldsymbol{\mu},\,\boldsymbol{\pi}) = p(\boldsymbol{X}|\boldsymbol{Z},\,\boldsymbol{\mu})p(\boldsymbol{Z}|\pi)p(\boldsymbol{\pi})p(\boldsymbol{\mu}) \tag{8}$$

The true posterior $p(\boldsymbol{Z}, \boldsymbol{\mu}, \boldsymbol{\pi}|\boldsymbol{X})$ is intractable to compute. But, as it is proportional to the joint distribution, we assume a mean field approximation of the variational posterior $p(\boldsymbol{Z}, \boldsymbol{\mu}, \boldsymbol{\pi}) = q(\boldsymbol{Z})q(\boldsymbol{\mu}, \boldsymbol{\pi})$. Then, using the expectation–maximization algorithm, we find the optimal variational parameters [39].

We determined the optimal number of clusters K by comparing the Evidence Lower Bound (ELBO) between values $K \in \{2, 3, \ldots, 8\}$ [40]. In variational inference, the ELBO serves as a tractable lower bound on the marginal log-likelihood and naturally incorporates model complexity penalties through the Kullback–Leibler divergence $\mathbb{KL}(\cdot||\cdot)$ between the variational posterior $q(\boldsymbol{Z})$ and the prior $p(\boldsymbol{Z}|\boldsymbol{\pi})$ [41]. It is specified as:

$$\mathcal{L}(q) = \mathbb{E}_q[\log p(\boldsymbol{X},\,\boldsymbol{Z})] - \mathbb{E}_q[\log q(\boldsymbol{Z})] = \sum_{n=1}^{N} \mathbb{E}_{q(z_n)}[\log p(\boldsymbol{x}_n|\boldsymbol{z}_n,\,\boldsymbol{\mu}] - \sum_{n=1}^{N} \mathbb{KL}(q(\boldsymbol{z}_n)||p(\boldsymbol{z}_n|\boldsymbol{\pi})) \tag{9}$$

For each value of K, we fit the model with 10 random initializations and selected the run achieving the highest ELBO to account for local optima in variational optimization. As shown in figure 3, the ELBO increased substantially from $K = 2$ to $K = 3$ and decreased from $K > 3$ (gains < 0.0), indicating diminishing returns. This pattern suggests that $K = 3$ achieves an optimal balance between model fitness and complexity.

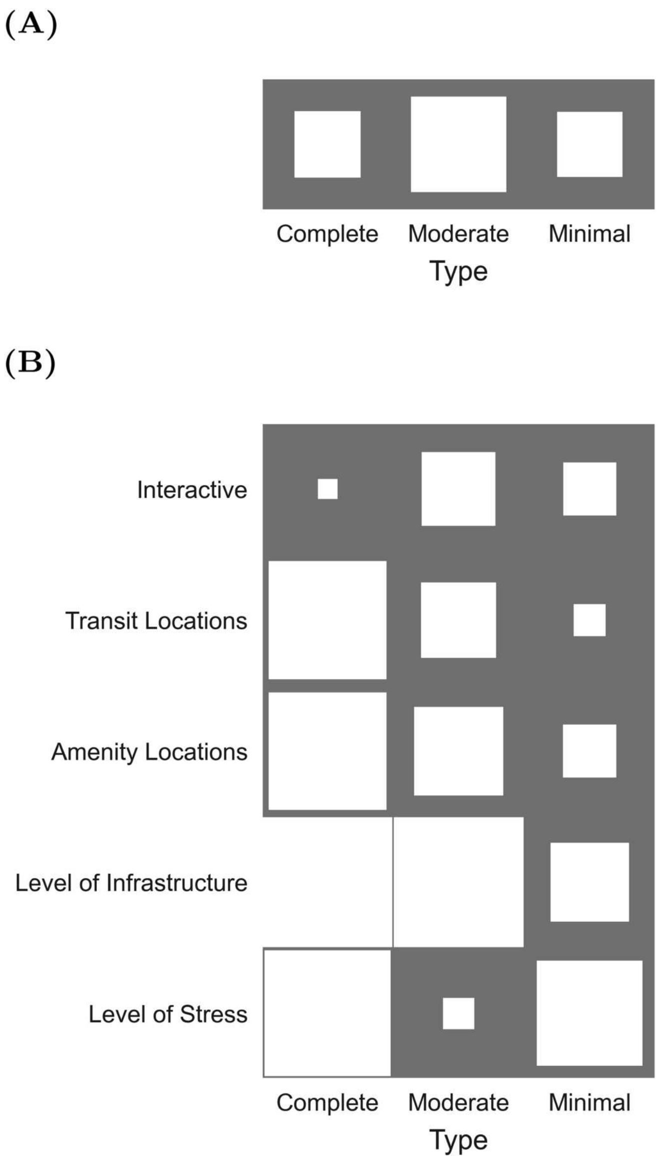

Figure 4. Hinton diagrams showing (A) the relative sizes of each map type cluster, and (B) the probability of each binary indicator being present within each map type. Square sizes are proportional to the values, providing a visual representation of the clustering structure that defines our three-type typology.

The posterior responsibilities are also obtained, by which we assign each observation $\boldsymbol{x}_n$ to each cluster k. The relative cluster sizes and indicator means μ_{dk} are shown via Hinton diagrams in figure 4.

2.5. Socioeconomic data and bicycle mode share model specifications

To examine associations between map characteristics and bicycle mode share, we fitted three models to predict bicycle mode share. Each model specification ($\mathcal{M}_1$, $\mathcal{M}_2$, and $\mathcal{M}_3$) included 14 socioeconomic variables but differed in terms of the map-related indicators. We collected the socioeconomic data from the 5-year American Community Survey (ACS) in 2023 [42]. These include population, median household income, vehicle ownership, and mode shares (portion of commuters by mode) for bicycling, walking, driving, and transit use. Land area data were also used to compute population density. A summary of the variables and model specifications is provided in table 1.

We selected explanatory variables in such a way as to capture both socioeconomic conditions and travel behaviors known to influence bicycle mode share. Population density captures built environment and urban form. Median household income reflects the economic conditions that affect travel choices. Household vehicle availability indicates transportation access and car dependency. Finally, commute mode shares for driving, transit, and walking represent complementary or competing modes that affect bicycling choices. These variables were obtained from the broader ACS dataset because they are consistently reported, interpretable across regions, and widely used in transportation research. Overall, these variables also served as controls to isolate the association between map-related features and bicycling activity. Scatter plots showing the relationships between bicycle mode share and each of the explanatory variables are presented in appendix A.3.

Table 1. County-level variables used in the predictive models and their inclusion across model specifications.

Category	Variable	$\mathcal{M}_1$	$\mathcal{M}_2$	$\mathcal{M}_3$
Socioeconomic (ACS)	0 Vehicles Available (proportion)	✓	✓	✓
	1 Vehicle Available (proportion)	✓	✓	✓
	2 Vehicles Available (proportion)	✓	✓	✓
	3+ Vehicles Available (proportion)	✓	✓	✓
	Households (count)	✓	✓	✓
	Land Area (sq mi)	✓	✓	✓
	Median Household Income ($)	✓	✓	✓
	Population Density (sq mi)	✓	✓	✓
	Total Workers (count)	✓	✓	✓
Commute Mode Shares (ACS)	Carpool Mode Share	✓	✓	✓
	Drove Alone Mode Share	✓	✓	✓
	Public Transit Mode Share	✓	✓	✓
	Walk Mode Share	✓	✓	✓
	Work from Home Mode Share	✓	✓	✓
Map Characteristics	Availability	✓	—	—
	Type (*Minimal, Moderate, Complete*)	—	✓	—
	Level of Infrastructure	—	—	✓
	Level of Stress	—	—	✓
	Amenity Locations	—	—	✓
	Transit Locations	—	—	✓
	Interactive	—	—	✓
Target variable	Bicycle Mode Share	✓	✓	✓

Table 2. Performance of the selected model (XGBoost) across the three specifications predicting bicycle mode share.

Mod. spec.	Counties	R^2_{train}	R^2_{test}	$\text{RMSE}_{\text{train}}$	$\text{RMSE}_{\text{test}}$	$\text{MAE}_{\text{train}}$	MAE_{test}
$\mathcal{M}_1$	684	0.8460	0.4493	0.0017	0.0049	0.0011	0.0025
$\mathcal{M}_2$	307	0.7835	0.4873	0.0030	0.0060	0.0016	0.0032
$\mathcal{M}_3$	307	0.9882	0.5809	0.0007	0.0054	0.0004	0.0031

2.6. Model selection and explanation

For each model specification, we assessed the performance of three supervised learning algorithms: ordinary least squares (OLS), random forests (RF)[43], and extreme gradient boosting (XGBoost) [44]. In the case of the RF and XGBoost algorithms, we used three-fold cross-validation to optimize the hyperparameters. XGBoost achieved the best out-of-sample performance across all specifications, and thus it was our algorithm of choice for each model specification. We summarize the performance of all the algorithms across the specifications in table 2. Furthermore, we provide grid search results, fold-level scores, learning/validation curves, optimal parameters and a comprehensive comparison of the algorithms in appendix A.1. We used the optimal hyperparameters obtained from the grid searches to fit the final models, $\mathcal{M}_1$, $\mathcal{M}_2$ and $\mathcal{M}_3$, for prediction and interpretation.

We then used SHapley Additive exPlanations (SHAP) to quantify individual feature contributions and their relative importance to model predictions [45]. Each SHAP value, ϕ_{nd}, represents the marginal impact of each feature d across all possible subsets $\mathcal{S}$ of input features in county n. It is specified as:

$$\phi_{nd} = \sum_{\mathcal{S}\subseteq\setminus\{d\}} \frac{|\mathcal{S}|!(D-|\mathcal{S}|-1)!}{D!}\left[\hat{f}(\boldsymbol{x}_{n\mathcal{S}} \cup \{x_{nd}\}) - \hat{f}(\boldsymbol{x}_{n\mathcal{S}})\right] \tag{10}$$

where $\hat{f}$ is the fitted model and $\boldsymbol{x}_{n\mathcal{S}}$ is the nth observation vector of features in subset $\mathcal{S}$. Positive SHAP values indicate features that increase predicted bicycle mode share and negative values indicate the opposite. Feature importance is assessed through the average magnitude of SHAP values across observations, $\frac{1}{N}\sum_n|\phi_{nd}|$.

3. Results

3.1. Three urban bicycle map types discovered

From the Bernoulli mixture model, we identified three distinct map types, namely, *Complete*, *Moderate*, and *Minimal*. *Minimal* maps (22% of available maps, $N = 68$) mainly feature level of stress information, focusing on route safety and

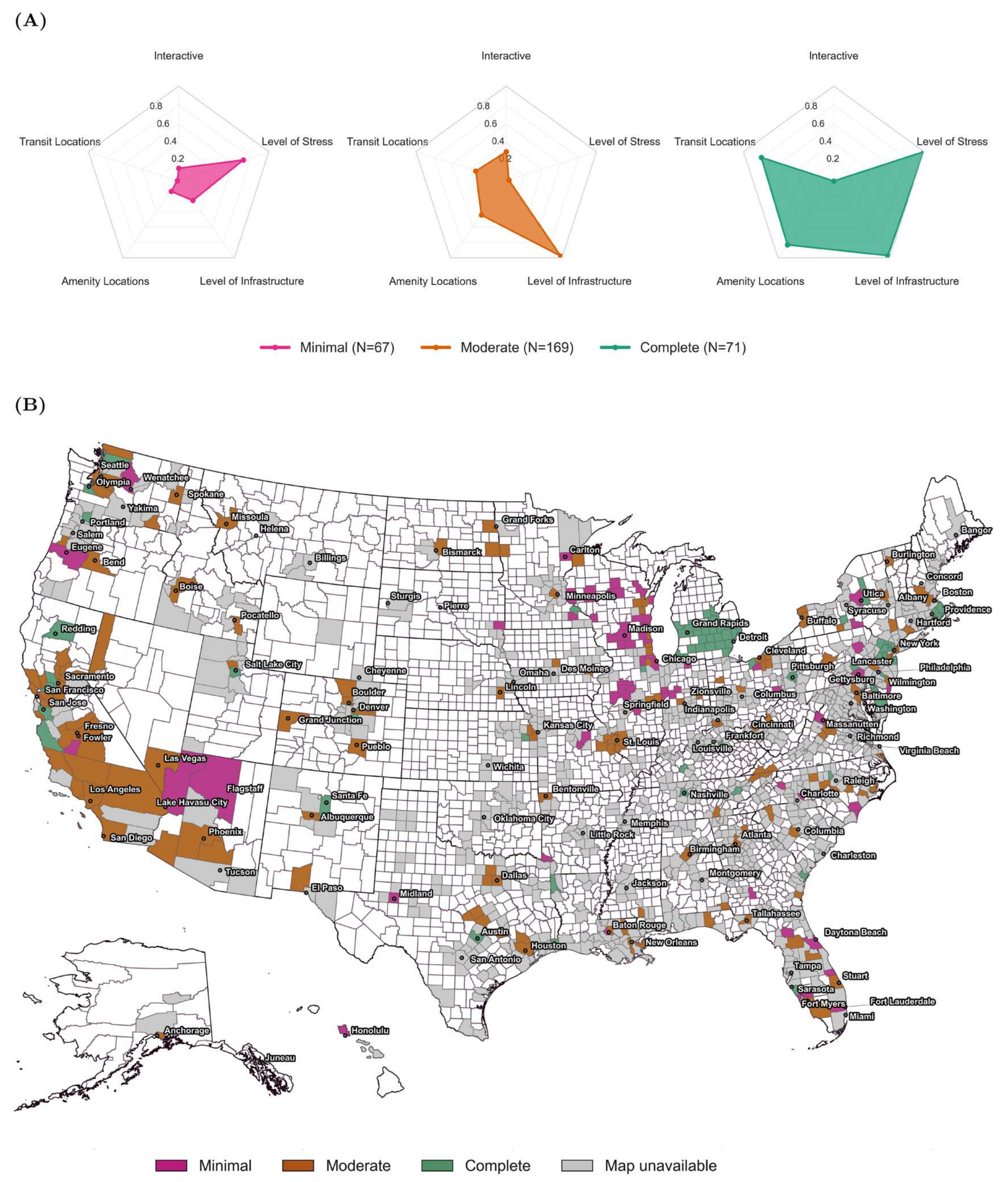

Figure 5. (A) Radar plots comparing features across bicycle map types. (B) Map of urban US counties showing the 3 bicycle map types. Counties in gray had no online maps. Content reflects bicycle maps available as of May 2025.

comfort rather than comprehensive infrastructure details. A few cities in counties of this type include Chicago, Eugene, Fort Lauderdale, and Madison. *Moderate* maps constitute the largest category (54%, $N = 167$) and consistently include the level of infrastructure information, indicating this as the dominant and most valued characteristic among map creators. These maps focus primarily on showing the physical bicycling infrastructure available to users. Prominent cities in counties of this type include Baltimore, Boise, Las Vegas, Los Angeles, Phoenix, and St. Louis. Finally, *Complete* maps (24%, $N = 72$) feature comprehensive information including transit and amenity locations, infrastructure details, and stress level indicators. These maps are predominantly found in the Northeast, West Coast, and Upper Midwest regions. Notable cities in counties of this type include Austin, Detroit, Nashville, Portland, San Francisco, and Seattle. The spider plot in figure 5(A) illustrates the average indicator values for each type, while figure 5(B) shows the geographic distribution of the underlying counties in the sample. Representative maps from each type are shown in figure 6.

3.2. Map availability is positively associated with bicycle usage

Counties with readily available bicycle maps demonstrate substantially higher bicycle mode shares than those without maps. As shown in figure 7(A), the mean bicycle mode share in counties with maps (0.49%) is nearly

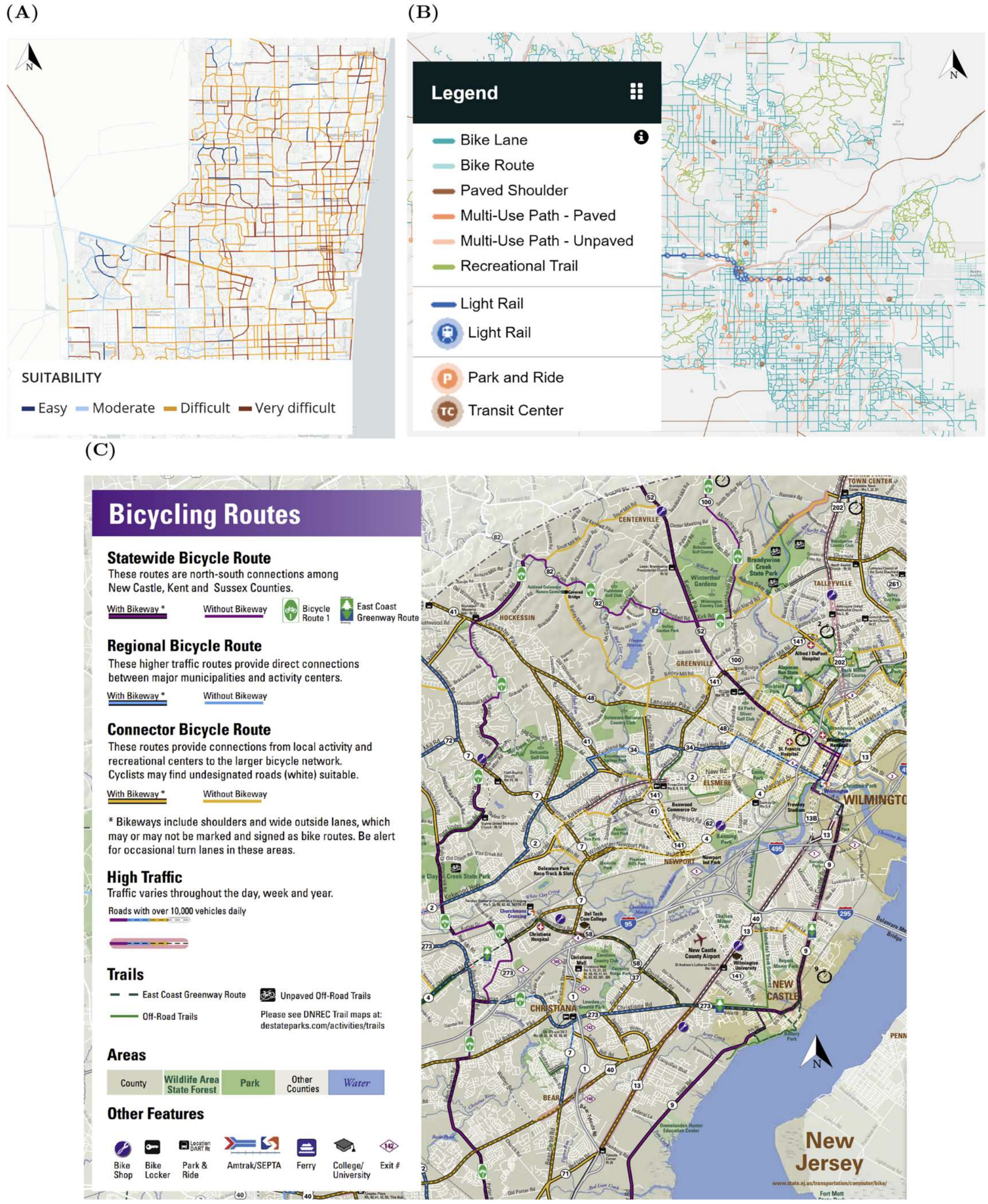

Figure 6. Representative maps and legends highlighting visual and informational elements associated with each map type: (A) *Minimal* (Broward County, FL), (B) *Moderate* (Maricopa County, AZ), and (C) *Complete* (New Castle, DE).

three times that of counties without maps (0.18%), representing a statistically significant difference ($t = 7.55, p < 10^{-12}$). This suggests a strong association between map availability and bicycling activity. Furthermore, the SHapley Additive exPlanation (SHAP) values of the bicycle mode share prediction model ($\mathcal{M}_1$, $R^2_{\text{test}} \approx 0.45$, figure 7(B)) showed that map availability is not only a moderately important predictor but also has a positive relationship with bicycle usage (figure 7(C)).

3.3. Complete maps are associated with lower bicycle usage

We also find that the bicycle map type in a given county also has explanatory power in predicting bicycle usage (figure 8(A)). *Complete* is the most important of the three type indicators. However, its effect is negative, suggesting that bicycle maps with the greatest amount of information tend to be associated with lower levels of bicycle usage. In contrast, *Minimal* maps (second most important) demonstrate a positive association with higher bicycling rates, indicating that simpler maps are more prevalent in areas with greater bicycle usage. The

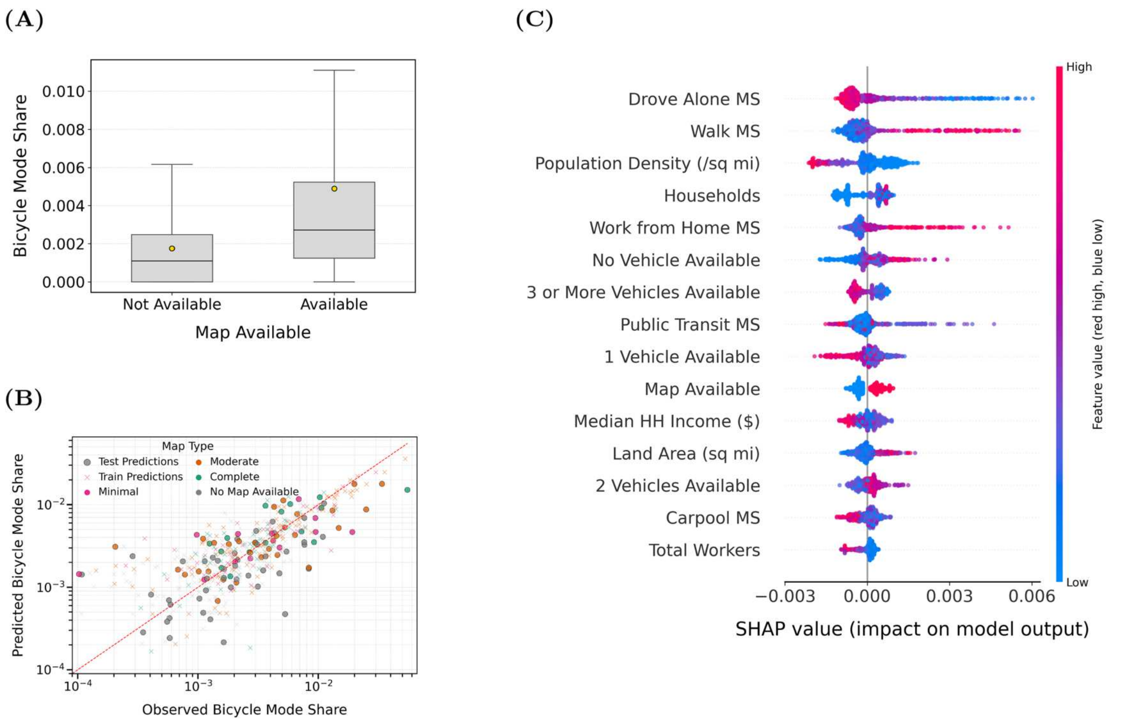

Figure 7. Bicycle mode share and predictive performance for counties with and without bicycle maps (Model $\mathcal{M}_1$). (A) Distribution of bicycle mode share comparing counties with and without available maps. (B) Observed versus predicted bicycle mode share ($R^2_{\text{test}} \approx 0.45$). (C) SHAP summary plot showing the contribution and relative importance of each input variable in predicting mode share. Feature effects are shown in order of influence.

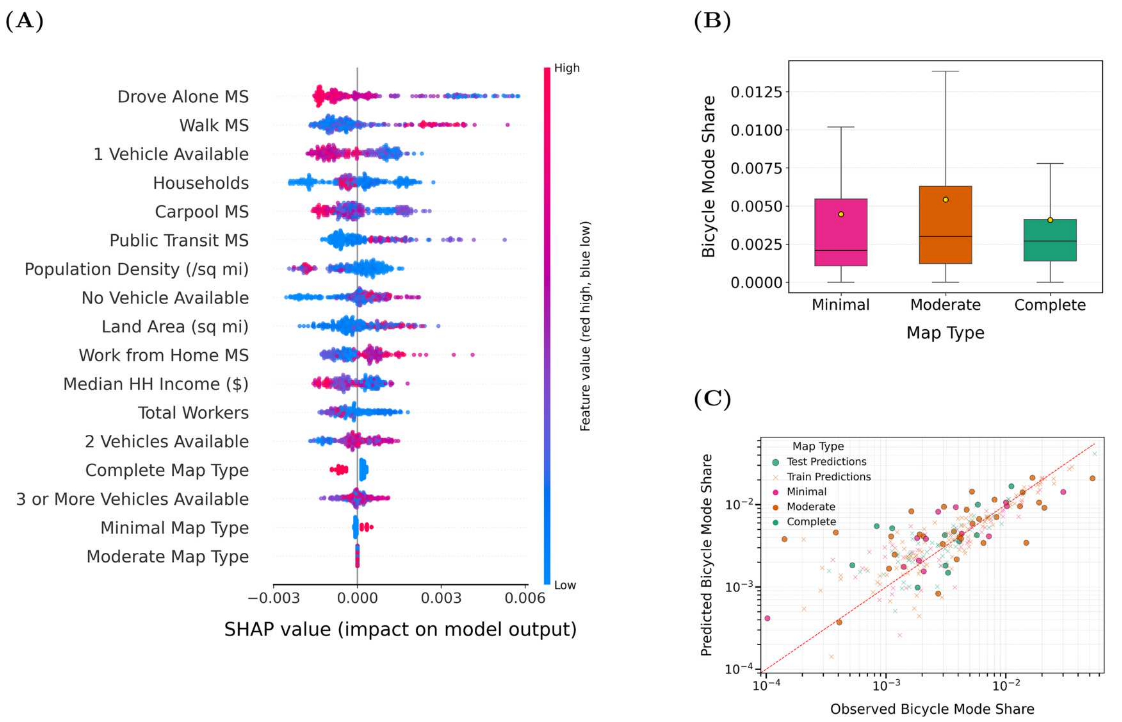

Figure 8. Bicycle mode share and predictive performance for different map types (Model $\mathcal{M}_2$): (A) SHAP summary plot showing the contribution and importance of each variable including map types in predicting bicycle mode share. (B) Distribution of bicycle mode share across the three map types. (C) Observed versus predicted bicycle mode share for the fitted model ($R^2_{\text{test}} \approx 0.48$).

distribution of bicycle mode share values by type (figure 8(B)) provides further insights. Counties with *Moderate* maps have the highest mean bicycle mode share (0.54%), followed by *Minimal* maps (0.45%) and *Complete* maps (0.41%).

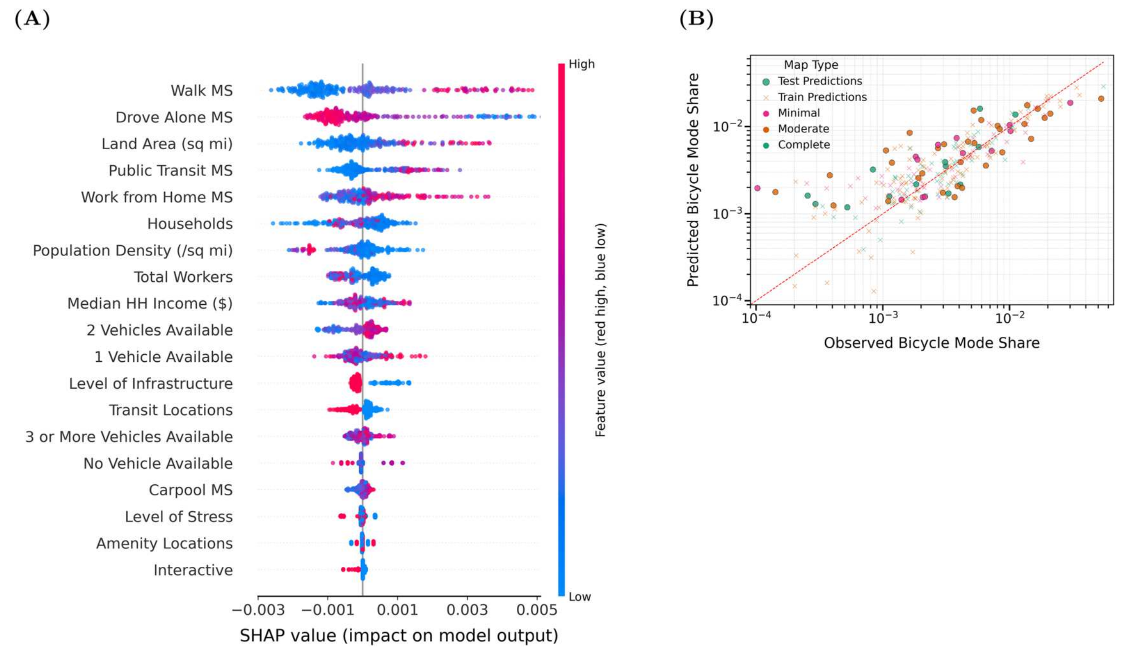

Figure 9. Bicycle mode share and predictive performance for counties with bicycle maps (Model $\mathcal{M}_3$): (A) Observed versus predicted bicycle mode share ($R^2_{\text{test}} \approx 0.58$). (B) SHAP summary plot showing the contribution and importance of each variable to the prediction.

3.4. Infrastructure and transit features are associated with lower bicycle usage

Finally, when we use the features in place of the type indicators as the map characteristics in the model ($\mathcal{M}_3$), we find that the most important map features for predicting bicycle usage are *Level of Infrastructure* and *Transit Locations* (figure 9(A)). However, both features demonstrate negative SHAP contributions, indicating that counties with maps having these features tend to have lower bicycle mode shares. The less important map features show mixed effects, except for *Interactive*, which is also negative. We also note that we obtain greater explanatory power when map features are used in place of the map type for predicting bicycle usage ($R^2_{\text{test}} \approx 0.58$ for $\mathcal{M}_3$ compared to $R^2_{\text{test}} \approx 0.48$ for $\mathcal{M}_2$).

4. Discussion

4.1. Map gap a potential barrier to bicycle usage in urban US

There is a significant gap in urban map availability, as only 45% of the counties sampled had a dedicated bicycle map available online. This presents an urgent need. It also potentially indicates that the effect of the availability of well-designed maps may have been under-emphasized in efforts to improve bicycle adoption [46]. One might argue that merely having good bicycling infrastructure is not enough to propel usage if bicyclists (or would-be bicyclists) do not have ready access to information that facilitates its use. Furthermore, the fact that map availability is positively associated with bicycle mode share indicates that map production in more counties could potentially contribute to increased bicycle usage. Map availability may also signal agency support for bicycling, which can shape intent and use [47–49].

4.2. Map characteristics are relevant to bicycle usage

Across the three model specifications we investigated for predicting bicycle mode share, performance ranged from moderate to strong (test $R^2 \approx 0.45$–0.58). This suggests that map-related variables add a useful signal beyond standard socioeconomic explanatory variables. Furthermore, these effects of these variables were consistent with regard to expectations from prior transportation research. For instance, population density and walking are positively associated with bicycling, while car availability and driving mode share are negatively associated [50–53].

4.3. Information overload could explain why bicycle maps with more detail are not always better

The *Complete* map type, which features the most detail, demonstrated a negative association with bicycle mode share. In addition, the SHAP results from $\mathcal{M}_3$ indicate that *Level of Infrastructure* and *Transit Locations*, which are the most relevant of the five map features in predicting bicycle usage, have a negative impact on bicycle usage. One possible explanation of this outcome is the effect of information or cognitive overload, which could be a result of map complexity [32, 54, 55]. Users may find maps depicting several layers, symbols, and points of interest difficult to read, interpret or use, which could in turn reduce the practical value of the map for everyday trips [29]. While there is no clear evidence in the literature as to whether visual map complexity degrades efficiency [29], this study provides initial empirical evidence for this possibility, particularly in the US context. Another untested hypothesis is that counties with lower rates of bicycling tend to design more feature-rich maps as a means of boosting ridership—a case of reverse causality [56, 57]. However, the investigation of causal relationships would require careful longitudinal study, which is outside the scope of this paper but could be a subject for future research.

4.4. Simple and accessible bicycle maps as a low-cost intervention for greater sustainability

Overall, our findings suggest that well-designed maps could serve as a low-cost lever to complement infrastructure interventions. In practice, this could mean producing a map with a clear layout that highlights only the most relevant features for wayfinding (e.g., stress, comfort and core facilities) rather than one that tries to show everything at once. From a policy perspective, improving access (readily accessible links, mobile-friendly formats) and simplifying design (legible symbology, concise legends, limited layers) are near-term steps that agencies can take alongside capital-intensive projects. These changes are inexpensive, relatively quicker to implement, and can be iterated based on feedback. Ultimately, they could yield increases in bicycle usage, which in turn would further contribute to environmental sustainability, as short-distance trips undertaken by cars shift to bicycles [4].

4.5. Study limitations and future directions

First, we note that this is an observational, cross-sectional study at the county level. Therefore, results may reflect unobserved factors such as the extent and quality of infrastructure, bike share systems, topography, or weather. Second, map publication dates were inconsistently reported. Thus we could not control for map age. This could potentially bias results if newer maps differ systematically from older ones.

In addition, the map indicators were labeled by visual inspection. Although results were produced and checked via two independent assessments, there is a potential for some measurement error. We also note that while commute mode share is a strong indicator of bicycle usage, this target variable does not always account for recreational or non-commute usage, which is not always insignificant. Finally, these results are based on a significant sample of urban counties in the US. Further research would be required to determine if they generalize to rural areas (which tend to be less dense) or to other countries with varying bicycle usage outcomes.

The consideration of temporal factors (map age, update history among others) could provide more explainability to model results. Computing the inter-coder agreement (ICA) in future studies such as this one would better quantify consistency of map labeling and improve data reliability. Longitudinal studies and natural experiments, where feasible, could provide evidence to properly test hypotheses regarding the impact of maps (in terms of availability and detail) on bicycle usage and vice versa.

5. Conclusion

A survey of 684 urban counties in the US indicated that only 45% have publicly available bicycle maps online. Analyzing the 307 available maps yielded five key features. Via a Bernoulli mixture model, we identified three distinct map types based on these. *Minimal* maps (22%) primarily display level of stress information, indicating traffic conditions and route difficulty. *Moderate* maps (54%) focus on the level of infrastructure. *Complete* maps (24%) include both infrastructure and stress information plus locations of transit stops and bicycling amenities.

We fitted multiple models to predict bicycle mode share based on socioeconomic factors and various map-related indicators. The models yielded the following insights. First, map availability is a significant predictor of bicycle usage and has a positive impact. Second, *Complete* maps are associated with lower bicycle usage, while the reverse is the case for *Minimal* maps. Third, of the five features, *Level of Infrastructure* and *Transit Locations* are the most relevant and are also associated with lower bicycle usage.

Overall, our findings indicate that more bicycle maps may be needed to encourage bicycling across the US. Furthermore, simpler maps which prioritize route stress information, may yield better outcomes than those with more features. Our methodological approach is generalizable and readily applicable to other settings.

Funding

The authors confirm that there were no conflicts of interest. This project was supported in part by an NSF Research Experiences for Undergraduates (REU) site program under Grant No. 2243853, and also by NSF Grant No. 2325956.

Data availability statement

The data that support the findings of this study are openly available at the following URL/DOI: https://github.com/narslab/bike-map-typology.git.

Appendix

A.1. Model selection

This section documents the full model-selection analyses. We (i) report the hyperparameter grids used for XGBoost and random forest and the configuration for OLS, (ii) summarize the best settings identified by cross-validation (CV) together with fold-level scores, and (iii) include training/validation learning curves for the selected XGBoost models. The comparison of the selected model across the specifications is provided in table 2.

Table 3 shows the hyperparameter grids that were used for tree-based models and the scaled pipeline for OLS (no hyperparameters).

Table 4 shows the optimal hyperparameter values for each specification and model.

We tune each model's hyperparameters via 3-fold cross-validation and select the final algorithm for each specification based on the held-out test performance. Table 5 reports the validation R^2 scores from the held-out fold for all model specifications and algorithms.

Table 6 shows the train/test performance for each model under each specification. XGBoost outperforms Random Forest and OLS across all three specifications based on the three metrics shown. Therefore, we selected it for the remainder of the analyses.

For each specification, we fit the selected model on an 80/20 train–test split. Figure 10 shows the training/validation curves, which indicate stable convergence.

Table 3. Search grids and configurations (shared across specifications unless noted).

Model and spec	Parameter	Values
XGBoost ($\mathcal{M}_1$, $\mathcal{M}_2$)	Number of trees	$\{150, 250, 350\}$
	Maximum tree depth	$\{2, 3, 4, 5, 8\}$
	Minimum child weight	$\{5, 10, 20, 30\}$
	Row subsample ratio	$\{0.7, 0.8, 1.0\}$
	Column subsample ratio (per tree)	$\{0.6, 0.8, 1.0\}$
XGBoost ($\mathcal{M}_3$)	Number of trees	$\{10, 15, 20, 30, 50, 100\}$
	Maximum tree depth	$\{4, 8, 10\}$
	Minimum child weight	$\{1, 5, 10\}$
	Learning rate	$\{0.3, 0.8, 1.0\}$
	Row subsample ratio	$\{0.7, 0.8, 1.0\}$
Random Forests ($\mathcal{M}_1$, $\mathcal{M}_2$, $\mathcal{M}_3$)	Number of trees	$\{300, 600\}$
	Maximum tree depth	$\{\text{None}, 10, 20\}$
	Min. samples to split a node	$\{2, 5\}$
	Min. samples at a leaf	$\{1, 2\}$
	Features considered per split	$\{\ \sqrt{\cdot}, 0.8\ \}$
OLS (all)	Pipeline	`[StandardScaler, LinearRegression]`
	Tunable hyperparameters	None

Table 4. Best settings (by CV R^2) with human-readable hyperparameter names.

Model spec	Algorithm	Hyperparameter	Optimal value
$\mathcal{M}_1$	XGBoost	Number of trees	150
		Maximum tree depth	2
		Minimum child weight	30
		Row subsample ratio	0.8
		Column subsample ratio (per tree)	0.6
	Random Forest	Number of trees	300
		Maximum tree depth	10
		Min. samples to split a node	5
		Min. samples at a leaf	2
		Features considered at each split	0.8
	OLS	No hyperparameters	Scaled pipeline
$\mathcal{M}_2$	XGBoost	Number of trees	150
		Maximum tree depth	2
		Minimum child weight	20
		Row subsample ratio	0.7
		Column subsample ratio (per tree)	0.8
	Random Forest	Number of trees	300
		Maximum tree depth	20
		Min. samples to split a node	2
		Min. samples at a leaf	2
		Features considered at each split	$\sqrt{\cdot}$
	OLS	No hyperparameters	Scaled pipeline
$\mathcal{M}_3$	XGBoost	Number of trees	30
		Maximum tree depth	4
		Minimum child weight	10
		Learning rate	0.3
		Row subsample ratio	0.8
		Column subsample ratio (per tree)	—
	Random Forest	Number of trees	300
		Maximum tree depth	10
		Min. samples to split a node	5
		Min. samples at a leaf	2
		Features considered at each split	$\sqrt{\cdot}$
	OLS	No hyperparameters	Scaled pipeline

Table 5. Fold-level cross-validation (CV) R^2 scores.

		R^2 by fold				
Model Spec.	Algorithm	Fold 1	Fold 2	Fold 3	Mean CV R^2	SD
$\mathcal{M}_1$	XGBoost	0.4405	0.3445	0.3930	0.3927	0.0394
	Random Forest	0.3868	0.4694	0.5026	0.4530	0.0491
	OLS	0.2769	0.1991	0.3969	0.2910	0.0813
$\mathcal{M}_2$	XGBoost	0.3781	0.3067	0.3446	0.3431	0.0291
	Random Forest	0.4931	0.2790	0.3171	0.3631	0.0955
	OLS	0.2698	0.2124	−0.3516	0.0435	0.2804
$\mathcal{M}_3$	XGBoost	0.4478	0.3108	0.2831	0.3472	0.0858
	Random Forest	0.4670	0.2680	0.3348	0.3566	0.0817
	OLS	0.2700	0.2058	−0.3867	0.0297	0.2956

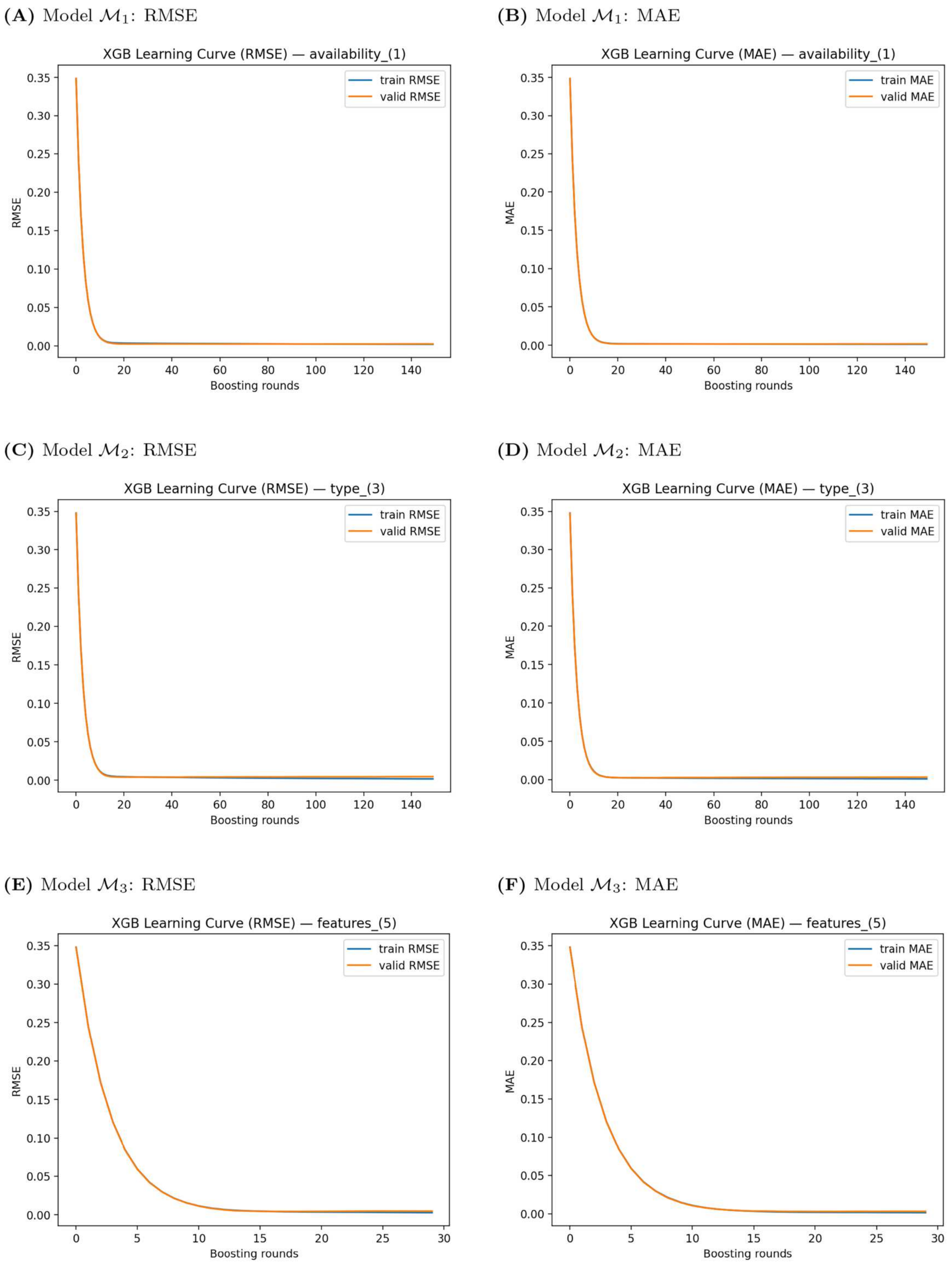

Figure 10. XGBoost training/validation learning curves (RMSE and MAE) for the selected models in each specification.

Table 6. Model performance across specifications. Train/test metrics are averaged across folds. Bolded rows indicate the best-performing algorithm per model specification.

Mod. spec.	Alg.	Counties	R^2_{train}	R^2_{test}	$RMSE_{train}$	$RMSE_{test}$	MAE_{train}	MAE_{test}
$\mathcal{M}_1$	OLS	684	0.1257	0.0439	0.0044	0.0064	0.0034	0.0039
	RF	684	0.9251	0.2623	0.0013	0.0057	0.0007	0.0026
	XGB	**684**	**0.8460**	**0.4493**	**0.0017**	**0.0049**	**0.0011**	**0.0025**
$\mathcal{M}_2$	OLS	307	0.0967	0.3361	0.0061	0.0068	0.0051	0.0057
	RF	307	0.7776	0.4406	0.0030	0.0063	0.0016	0.0032
	XGB	**307**	**0.7835**	**0.4873**	**0.0030**	**0.0060**	**0.0016**	**0.0032**
$\mathcal{M}_3$	OLS	307	0.0862	0.3138	0.0062	0.0069	0.0051	0.0058
	RF	307	0.7984	0.4721	0.0029	0.0061	0.0014	0.0032
	XGB	**307**	**0.9882**	**0.5809**	**0.0007**	**0.0054**	**0.0004**	**0.0031**

A.2. Coding guide for map indicators

Table 7 summarizes the reference guide used to ensure consistency when categorizing map features as 1 (present) or 0 (absent).

Table 7. Definitions and examples used in categorizing the five binary map indicators.

Indicator	Definition	Example legend items
Level of Infrastructure	Distinguishes between different facility types	Protected bike lane Buffered lane Shared route Color-coded infrastructure types
Level of Stress	Indicates route comfort, difficulty, or traffic stress level	Low stress route High stress Preferred route Color-coded stress ratings
Amenity Locations	Shows bicycle-related amenities	Wrench icon Bike shop Repair station Bike parking
Transit Locations	Displays transit connections	Bus or train symbol Transit hub Metro line
Interactive	Includes web-based features allowing user interaction	Interactive web map Selectable layers Zoom or route-planning controls

A.3. Data exploration

Figure 11 provides a comprehensive view of the bivariate relationships between each predictor variable and bicycle mode share across different map types.

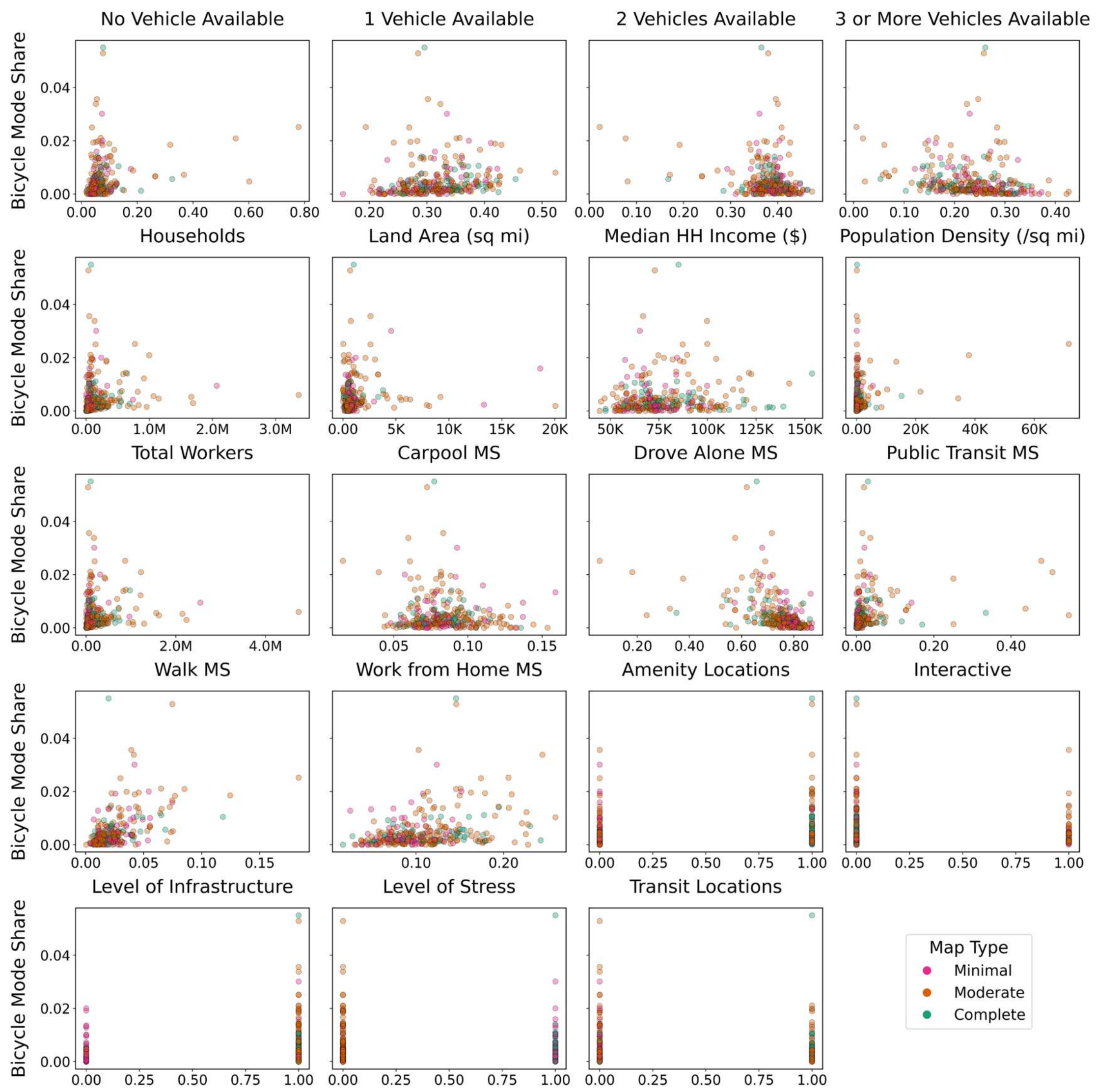

Figure 11. Scatter plots showing bicycle mode share versus all study variables, with points colored by map type (*Minimal*, *Moderate*, *Complete*).

Author contributions

Geehan Altayb 0009-0000-7203-1170
Conceptualization (supporting), Data curation (equal), Software (supporting), Writing – original draft (supporting)

Eleni Christofa 0000-0002-8740-5558
Investigation (supporting), Methodology (supporting), Supervision (supporting), Writing – review & editing (supporting)

Jimi Oke 0000-0001-6610-445X
Conceptualization (lead), Data curation (supporting), Formal analysis (lead), Funding acquisition (lead), Investigation (lead), Methodology (lead), Project administration (lead), Software (equal), Supervision (lead), Visualization (equal), Writing – original draft (lead), Writing – review & editing (lead)

References

[1] Green S, Sakuls P and Levitt S 2021 Cycling for health: improving health and mitigating the climate crisis *Canadian Family Physician Medecin De Famille Canadien* **67** 739–42

[2] Brand C *et al* 2021 The climate change mitigation effects of daily active travel in cities *Transportation Research Part D: Transport and Environment* **93** 102764

[3] Brand C, Dekker H J and Behrendt F 2022 Chapter eleven - cycling, climate change and air pollution *Advances in Transport Policy and Planning* **10** 235–64

[4] Chen W *et al* 2022 Historical patterns and sustainability implications of worldwide bicycle ownership and use *Communications Earth & Environment* **3** 171

[5] Oke O, Bhalla K, Love D C and Siddiqui S 2015 Tracking global bicycle ownership patterns *Journal of Transport & Health* **2** 490–501

[6] Pucher J and Buehler R 2008 Making cycling irresistible: lessons from The Netherlands, Denmark and Germany *Transport Reviews* **28** 495–528

[7] League of American Bicyclists. National: Rates Of Biking & Walking 2026 https://data.bikeleague.org/data/national-rates-of-biking-and-walking

[8] Jiang K, Yang Z, Feng Z, Yu Z, Bao S and Huang Z 2019 Mobile phone use while cycling: a study based on the theory of planned behavior *Transportation Research Part F: Traffic Psychology and Behaviour* **64** 388–400

[9] Caballero R *et al* 2019 Using the theory of planned behavior to explain cycling behavior *Avances en Psicología Latinoamericana* **37** 283–94

[10] Cai S, Long X, Li L, Liang H, Wang Q and Ding X 2019 Determinants of intention and behavior of low carbon commuting through bicycle-sharing in China *J. Clean. Prod.* **212** 602–9

[11] Litman T A 2025 *Evaluating Accessibility for Transport Planning: Measuring People's Ability to Reach Desired Services and Activities* Victoria Transport Policy Institute Available at: https://www.vtpi.org/access.pdf

[12] Golledge R G 1999 *Wayfinding Behavior: Cognitive Mapping and Other Spatial Processes* (Johns Hopkins University Press)

[13] Guo Z 2011 Mind the map! The impact of transit maps on path choice in public transit *Transportation Research Part A: Policy and Practice* **45** 625–39

[14] Winters M *et al* 2012 Safe cycling: how do risk perceptions compare with observed risk? *Canadian Journal of Public Health* **103** S42–7

[15] Broach J, Dill J and Gliebe J 2012 Where do cyclists ride? A route choice model developed with revealed preference GPS data *Transportation Research Part A: Policy and Practice* **46** 1730–40

[16] Teschke K *et al* 2012 Route infrastructure and the risk of injuries to bicyclists: a case-crossover study *American Journal of Public Health* **102** 2336–43

[17] van Lierop D *et al* 2020 Wayfinding for cycle highways: assessing e-Bike users' experiences with wayfinding along a cycle highway in the Netherlands *Journal of Transport Geography* **88** 102827

[18] Haworth N, Delbosc A, Schramm A and Haslam N 2024 How might advertising campaigns Rehumanize cyclists? *Transportation Research Part F: Traffic Psychology and Behaviour* **105** 246–56

[19] Hu X, Chen Y, Xu S and Li S 2024 Exploring spatiotemporal interaction patterns of dockless shared bicycle networks: a case study of Shenzhen, China *ISPRS Annals of the Photogrammetry, Remote Sensing and Spatial Information Sciences* **X-4-2024** 169–74

[20] Zahertar A and Lavrenz S 2024 Impacts of spatiotemporal and COVID-19 factors on bike-share ride duration in detroit *Sustainability* **16** 7672

[21] Xiang Z, Li Q, Hong L, Sheng J and Ban P 2024 Effects of built environment on the spatio-temporal trajectories of shared bicycles: a case study of Shenzhen *Tropical Geography* **44** 236–47

[22] Vybornova A, Cunha T, Gühnemann A and Szell M 2023 Automated detection of missing links in bicycle networks *Geogr. Anal.* **55** 239–67

[23] Ermagun A, Erinne J and Maharjan S 2023 Equity of bike infrastructure access in the united states: a risky commute for socially vulnerable populations *Environmental Research: Infrastructure and Sustainability* **3** 035001

[24] Mölenberg F J M, Panter J, Burdorf A and van Lenthe F J 2019 A systematic review of the effect of infrastructural interventions to promote cycling: strengthening causal inference from observational data *International Journal of Behavioral Nutrition and Physical Activity* **16** 93

[25] Xiao C S, Sharp S J, van Sluijs E M F, Ogilvie D and Panter J 2022 Impacts of new cycle infrastructure on cycling levels in two french cities: an interrupted time series analysis *International Journal of Behavioral Nutrition and Physical Activity* **19** 77

[26] Reynolds C C, Harris M A, Teschke K, Cripton P A and Winters M 2009 The impact of transportation infrastructure on bicycling injuries and crashes: a review of the literature *Environmental Health* **8** 47

[27] League of American Bicyclists 2022 *Benchmarking Bike Networks* League of American Bicyclists Available at: https://bikeleague.org/sites/default/files/Benchmarking-Bike-Networks-Report-final.pdf

[28] Krizek K, Barnes G and Thompson K 2009 Analyzing the effect of bicycle facilities on commute mode share over time *J. Urban Plann. Dev.* **135** 66–73

[29] Büchel D and Reichenbacher T 2023 The visual complexity of bike maps *Proceedings of the ICA* **5** 1–8

[30] Wessel N and Widener M 2015 Rethinking the urban bike map for the 21st century *Cartographic Perspectives* 6–22

[31] Keil J, Edler D, Kuchinke L and Dickmann F 2020 Effects of visual map complexity on the attentional processing of landmarks *PLoS One* **15** e0229575

[32] Rymarkiewicz W, Cybulski P and Horbiński T 2024 Measuring efficiency and accuracy in locating symbols on mobile maps using eye tracking *ISPRS International Journal of Geo-Information* **13** 42

[33] Gao T, Daamen W, Krishnakumari P and Hoogendoorn S 2024 Map-matching for cycling travel data in urban area *IET Intel. Transport Syst.* **18** 2178–203

[34] Löw P S and Krisp J M 2024 Smoothing the ride: a surface roughness-centric approach to bicycle routing *AGILE: GIScience Series* **5** 1–6

[35] Pucher J, Buehler R and Seinen M 2011 Bicycling renaissance in North America? An update and re-appraisal of cycling trends and policies *Transportation Research Part A: Policy and Practice* **45** 451–75

[36] U.S. Census Bureau 2023 Office of Management and Budget (OMB) Bulletins Available at: https://www.census.gov/programs-surveys/metro-micro/about/omb-bulletins.html

[37] Oke J B *et al* 2019 A novel global urban typology framework for sustainable mobility futures *Environ. Res. Lett.* **14** 095006

[38] Moutounet-Cartan P G B 2020 A Bernoulli mixture model to understand and predict children longitudinal wheezing patterns arXiv:2005.02931

[39] Kaji D and Watanabe S 2011 Two design methods of hyperparameters in variational bayes learning for Bernoulli mixtures *Neurocomputing* **74** 2002–7

[40] Blei D M, Kucukelbir A and McAuliffe J D 2017 Variational inference: a review for statisticians *J. Am. Stat. Assoc.* **112** 859–77

[41] Wade S 2023 Bayesian cluster analysis *Philosophical Transactions of the Royal Society A: Mathematical, Physical and Engineering Sciences* **381** 20220149

[42] U.S. Census Bureau 2024 American Community Survey 5-Year Data (2009-2024) Available at: https://www.census.gov/data/developers/data-sets/acs-5year.html

[43] Breiman L 2001 Random forests *Mach. Learn.* **45** 5–32

[44] Chen T and Guestrin C 2016 XGBoost: a scalable tree boosting system *The 22nd ACM SIGKDD International Conference on Knowledge Discovery and Data Mining* (ACM) pp 785–94

[45] Lundberg S and Lee S I 2017 A unified approach to interpreting model predictions *The 31st International Conference on Neural Information Processing Systems* pp 4768–4777

[46] Pucher J, Dill J and Handy S 2010 Infrastructure, programs, and policies to increase bicycling: an international review *Preventive Medicine* **50** S106–25

[47] Aldred R, Watson T, Lovelace R and Woodcock J 2019 Barriers to investing in cycling: stakeholder views from England *Transportation Research Part A: Policy and Practice* **128** 149–59

[48] Chen X 2022 Predicting college students' bike-sharing intentions based on the theory of planned behavior *Frontiers in Psychology* **13** 836983

[49] Hull A and O'Holleran C 2014 Bicycle infrastructure: can good design encourage cycling? *Urban, Planning and Transport Research* **2** 369–406

[50] Parkin J, Wardman M and Page M 2008 Estimation of the determinants of bicycle mode share for the journey to work using census data *Transportation* **35** 93–109

[51] Dill J and Carr T 2003 Bicycle commuting and facilities in major US cities: if you build them, commuters will use them *Transportation Research Record: Journal of the Transportation Research Board* **1828** 116–23

[52] Pucher J and Buehler R 2006 Why canadians cycle more than americans: a comparative analysis of bicycling trends and policies *Transport Policy* **13** 265–79

[53] Zhou T, Feng T and Kemperman A 2023 Assessing the effects of the built environment and microclimate on cycling volume *Transportation Research Part D: Transport and Environment* **124** 103936

[54] Eppler M J and Mengis J 2004 The concept of information overload: a review of literature from organization science, accounting, marketing, MIS, and related disciplines *The Information Society* **20** 325–44

[55] Arnold M, Goldschmitt M and Rigotti T 2023 Dealing with information overload: a comprehensive review *Frontiers in Psychology* **14** 1122200

[56] Feng Q and Wu G L 2018 On the reverse causality between output and infrastructure: the case of China *Economic Modelling* **74** 97–104

[57] Khezri-nejad-gharaei M and Garcia-López MÀ. 2025 Reverse causality between urbanization and climate change *International Economic Journal* **39** 1–29